Synthesis and Characterization of spongy-ZnO for Photocatalytic Application

A Thesis Submitted
In Partial Fulfilment of the Requirement
For the degree of

BACHELOR OF TECHNOLOGY
(B. TECH.)

Submitted by:
Angelica Surin
Roll No. 111CR0112

Under the Supervision
of
Prof. Debasish Sarkar

DEPARTMENT OF CERAMIC ENGINEERING,
NATIONAL INSTITUTE OF TECHNOLOGY, ROURKELA
MAY 2015

CERTIFICATE

This is certified that the work enclosed in the project entitled "**SYNTHESIS AND CHARACTERIZATION OF SPONGY - ZnO FOR PHOTOCATALYTIC APPLICATION**" by Angelica Surin bearing Roll No. 111CR0112 in partial fulfilment of the requirements of the award of Bachelor of Technology Degree in Department of Ceramic Engineering at the National Institute of Technology, Rourkela is an authentic work carried out by her under my extreme guidance and supervision.

To the best of my acquaintance, the work embodied in the thesis has not been submitted to any other university / Institute for the award of any Degree or Diploma.

11/5/15

Debasish Sarkar

ASSOCIATE PROFESSOR
Department of Ceramic Engineering
National Institute of Technology
Rourkela-769008

ACKNOWLEDGEMENT

I am heartily grateful to Prof. Debasish Sarkar, Department of Ceramic Engineering, NIT, ROURKELA for his appreciated assistance and supervision in the accomplishment of this project work. I will always remain thankful for his methodical guidance as my instructor.

My deepest thanks to Sangeeta Adhikari for all the indescribable assistance and care she offered.

I also acknowledge all the members of ceramic engineering department for their recommendations and cooperation during this project work. I would like to express my wholehearted obligations to all my friends who constantly assisted me in the completion of this research project.

11/may/2015

Angelica Surin

Roll No.111CR0112

ABSTRACT

The use of nanostructured semiconductor for environmental issues has recently grabbed the attention of many eminent researchers. Photocatalysis via advance oxidation process helps in many of the global problems such as treatment of dye effluents, organic compounds, pathogens etc. ZnO is one such semiconductor inorganic material with an advantage of absorbing a large amount of solar spectrum in comparison to widely studied photocatalyst TiO_2. Thus, in this research work, we have carried to synthesize spongy-ZnO nanopowders by a simple, rapid and novel solution-combustion process using citric acid as an organic fuel and zinc nitrate hexahydrate as oxidant. The process optimization is carried by varying the molar ratio of oxidant to fuel and analysed them analytically in respect of crystallinity, morphology, crystal structure and surface area. Structural confirmation of spongy-ZnO has been carried by FT-IR spectral method whereas band gap energy is determined by UV-DRS spectroscopy. The photoactivity of the synthesized powders has been studied by degrading a model dye, methyl violet. Zinc oxide is observed to show high catalytic efficiency under visible light irradiation.

Table of Contents

List of Figures:

Chapter-1

Introduction

1.1 Background

Semiconductors are known to possess multiple properties for various functional applications. Some of the renowned semiconductors are TiO_2, ZnO, SnO_2, CdS, CdSe, WO_3 etc [1, 2]. Among the semiconductors mentioned, ZnO is one of the potential materials having multi-functional properties such as piezoelectric [3], optical [4], photochemical [5], optoelectronic [6] and electrical [7] sectors. Its applicability further explores as in the field of sensors [8], transducer [9] and efficient catalyst [10]. The energy band gap of ZnO is 3.2 eV. The band gap of ZnO is similar to TiO_2, which is a widely studied material. Annually, 1.2 million tonnes of zinc oxide is used in excess as depicted by a survey made by international zinc association. Figure 1 describes the world wide zinc oxide applications in various industrial sectors. The pie chart shows the maximum usage of ZnO is in rubber industry but some major applications also lie in ceramic and chemical industries. If we talk about the visible application, then it is present in the form of emulsion in skin care products such as creams, sunscreens, powders, etc. Recently, nanostructured zinc oxide is used for various electro-functional and photo-functional applications [11].

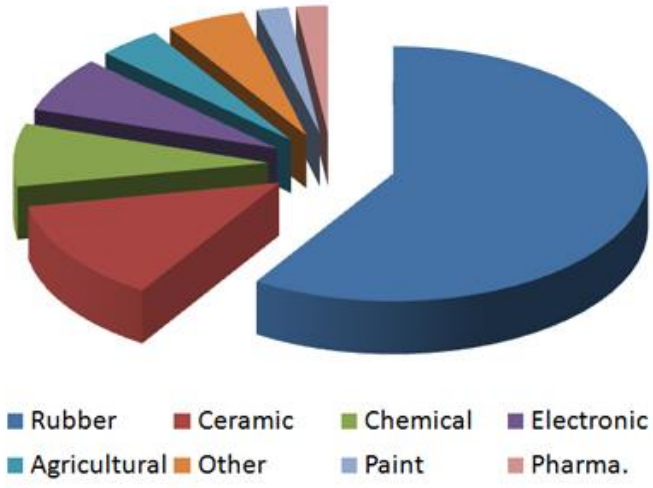

Figure 1. Usage of Zinc oxide in different industrial sectors.

1.2 Crystal Structure

ZnO has hexagonal wurtzite structure at room temperature and pressure. However, ZnO can contribute to three structural symmetries namely wurtzite, zinc blende and rock salt as shown in Figure 2. The zinc blende structure can be formed by the growth of ZnO in a cubic substrate. ZnO remains in a metastable state at high pressure bearing rocksalt type structure [12]. Figure 3 shows the hexagonal close packing sublattice that can hold either Zn or O atom [13]. Here each anion (O^{2-}) is surrounded by four cations (Zn^{2+}) at the corners of the tetrahedron and follows sp^3 hybridization for tetrahedral coordination between Zn^{2+} and O^{2-}.

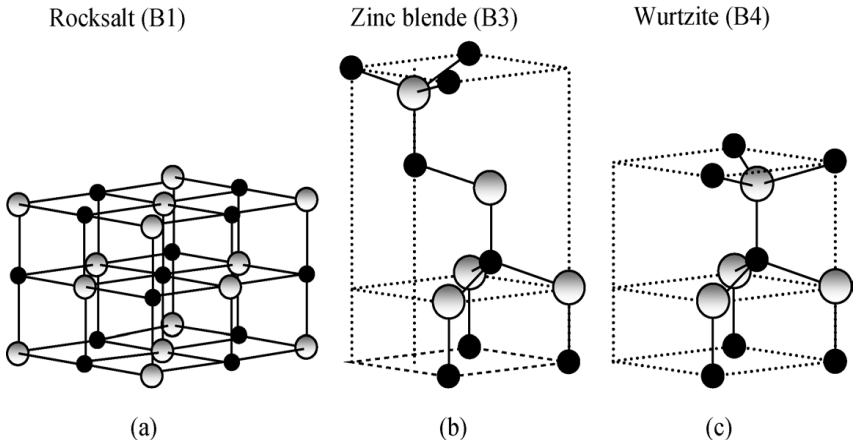

Figure 2. Different crystal structures of ZnO.

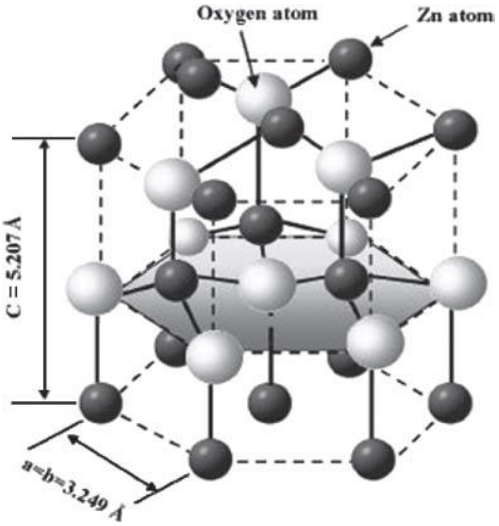

Figure 3. Hexagonal crystal structure of ZnO.

ZnO is non-symmetric in nature due to its tetrahedral coordination between cations and anions that are responsible for several piezoelectric and pyroelectric properties in its structure [14]. The optical properties of zinc oxide are based upon two emission bands that are short wavelength band near the fundamental absorption range and long wavelength band in green spectral range [15]. ZnO is a donor type semiconductor whose conductivity can be increased upon doping by other metals like Al, Gd, etc. Scientists are studying this particular material since decades as it is an alternate to TiO_2 in the field of photocatalysis.

1.3 Photocatalysis

In this process, the semiconductor material is being irradiated in the presence of photons. The photocatalyst should be cost effective, high efficient to use the light and also non-toxic in nature [16]. Semiconductors such as ZnO, TiO_2, Fe_2O_3 can act as sensitizers for light-induced redox-processes. The electronic structure of semiconductors has filled valance and conduction band. Upon irradiation to light the electron from valence band goes to conduction band creating holes. The holes react with the electron donor species or hydroxide ion to produce powerful oxidizing species like hydroxyl ion. Degradation of dye is done by this oxidizing species [17]. Figure 4 shows a typical mechanism for degradation of various organic compounds, textile dyes and others.

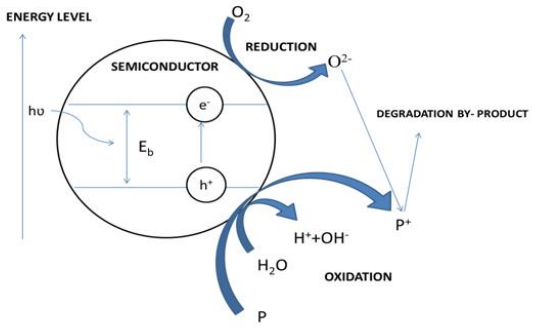

Figure 4. The schematic mechanism for photoactivity of semiconductors.

Chapter-2

Literature Review

ZnO is a versatile useful material but its functionality depends on the parameters like morphology, surface area and particle size. These parameters tend to depend on the various synthesis methods [18]. Synthesis methods like sol-gel, precipitation, hydrothermal, solvothermal, chemical vapour deposition, thermal decomposition, combustion method and electrophoretic deposition are available for the production of nanostructured ZnO particles [19]. Among the above techniques combustion synthesis is the most reliable and easy technique for production of ZnO nanoparticles. In this method redox reaction between fuel and oxidizer takes place with the evolution of various gaseous products. The heat generated during combustion process accompanying with greater mass loss leads to the formation of nanosized ZnO particle. Evolution of gaseous product limits the occurrence of agglomeration and may lead to a change in surface structures. A highly porous powder is prepared from this method having high crystallinity with pure phase that is required for photocatalytic application [20].

One of the researchers carried preparation of ZnO with different organic fuels namely β-alanine, valine, zinc acetate and acrylamide. The process takes place via self propagation reaction between zinc nitrate and various fuels. In case of β-alanine and valine the combustion reactions are quiet violent and takes place within seconds which causes significant weight loss. However, zinc acetate showed maximum yield without any significant loss. Zinc acetate has two major advantages; they are a less intense exothermic reaction and the yield was improved because of Zn^{2+} coming from both cation and anion. But, in case of acrylamide the mass loss occur at the much lower rate due to the formation of gel-like consistency. The ZnO synthesized using β-alanine gives the scaly appearance and viel like structure having less than 30 μm particles size whereas valine gives cavernous structure with 90 μm particle size. Zinc acetate and acrylamide gave rounded grains that are less than 15 μm in size. Different fuels and

different fuel to oxidizer ratio were taken producing different morphologies [21].

In another study, nanocrystalline ZnO powders were synthesized using glycine as a fuel. The combustion was carried out without the addition of water in zinc nitrate as zinc nitrate possess the property of hygroscopicity. The combustion preceded in three different modes: (i) SCS (smouldering combustion synthesis F/O ratio <1.05, combustion temperature Tc<650ºC). (ii) VCS (volume combustion synthesis) have F/O ratio in between 1.05-1.90 and combustion temperature is between 1000 ºC – 1250 ºC. (iii) SHS (self-propogating high temperature synthesis) F/O ratio is in between 850-1000 ºC. Morphologically, VCS showed a cluster of tiny particles with lose appearance whereas SHS showed the shard-like flake with holes. The powders obtained using SCS showed conglomerates composed of agglomerates of tiny particles. VCS and SHS give highly pure ZnO where as SCS showed the presence of an impurity in the crystal phase [22].

Potti et al did a comparative study of combustion-derived ZnO nanoparticles using fuels such as citric acid, dextrose, glycine, oxalyl di hydrazide, oxalic acid and urea followed by a study of their photocatalytic activity. The ZnO powders formed from the above fuel gives hexagonal wurtzite structure and ZnO crystalline size was found to be from 37-81 nm. Maximum absorption was observed in UV region. Strain in the catalyst increased with decreasing crystallite size. Different morphology was observed with different fuel combustion. The citric acid catalyzed ZnO produced particle with few surface pore whereas the dextrose catalyzed powders were irregular in shape with varied pore structure. ZnO prepared by glycine and oxalyl dihydrazide was found to have spherical shape particles. The powder prepared from the oxalic acid was cylindrical in shape but ZnO prepared using urea showed flower like ZnO structure. The ZnO nanocrystals prepared from oxalic acid showed high crystallinity, high surface area and showed the best photocatalytic activity towards the degradation and decolourization of azo dye namely orange G [23].

Another researcher studied the photocatalytic degradation of Rhodamine B dye under UV/solar light using ZnO nanopowder. In this study, combustion was carried using sugar as an efficient fuel. The crystallite size as calculated from XRD pattern was found to be 50 nm approximately. The SEM showed that particle synthesized have a uniform circular shape that are weakly agglomerated. Rhodamine B is a model dye and is widely used in textile industry and food stuffs. The dye effluent is carcinogenic in nature and also toxic beyond certain limits. The photocatalytic experiments were carried with respect to parameters like crystallite size, pH value, COD level and ZnO loading. On decreasing crystallite size of ZnO particles the photocatalytic activity was increased. The pH value of dye solution was varied using HCl or NaOH solution. The % degradation was minimum at pH 6.5-7.5 and high at alkaline pH values. The chemical oxygen reduction takes place at a faster rate under solar light than UV-light irradiation [24].

Recently, Adhikari et al synthesized hexagonal ZnO quasi-fibers using oxalic acid as a potential fuel. A clear demonstration on the formation of ZnO nanocrystals upon varying the oxidizer by fuel ratio, time and temperature was carried. High-resolution TEM images showed that the quasi-fibers consisted of agglomerated small spherical particles oriented in a single direction to produce fibers. The average size of the spherical particles is 50 nm. The optimized crystal was used for photocatalytic degradation of model dye methyl orange. High photo-efficiency was observed in UV light but there was not much difference in the photocatalytic efficiency of UV and Visible degradation. Moreover, particles were reused till four consecutive cycles without much degradation under visible light irradiation [25].

Sharma et al studied the influence of fuel and oxidizer ratio in lattice parameter and morphology of combustion synthesized powders. The synthesis of ZnO powders using urea as fuel is done via dry combustion synthesis. A combustion reaction can influence by various processing parameters such as (C/H ratio) type of fuel, fuel to oxidizer ratio (F/O), the water

content of precursor mixture and ignition temperature. The study regarding the structural aspect of ZnO was explored with variation in F/O ratio. An excellent correlation between an experimental pattern and the standard pattern was found to exist. High crystallinity was confirmed for ZnO powder with calculated and standard lattice parameter for hexagonal ZnO. The effect of urea on the ratio of lattice parameter shows that the variation in (c/a) ratio can be characterized by three domains. When the fuel content is in between 0.04-0.6, the crystal grows and attain pyramidal shape. For further increase in F/O it gets transformed into polycrystalline spherulites that on further increase scatter to attain sheet like morphology. Maximum F/O ratio leads to the evolution of the higher content of gaseous product that may lead to surface changes in structure [26].

In respect to the above literature and their findings three prime objective has been set as represented below:

Objective of the Work:

- To synthesize spongy-ZnO by one step solution-combustion method.
- To perform analytical characterization of the synthesized powders and analyze.
- To perform the photocatalytic degradation of methyl violet under visible and solar light irradiation.

Chapter-3

Experimental

Procedures

3.1. Synthesis of spongy-ZnO

- Raw materials used:
    - ✓ Zinc nitrate hexahydrate
    - ✓ Citric acid

The ZnO nanocrystals are derived from solution-combustion synthesis method. According to this method, the stoichiometric molar ratio of citric acid and zinc nitrate hexahydrate was taken in crystallization dish and dissolved in the minimum amount of distilled water to form a clear solution. Here, citric acid has been used as a combustion fuel. The clear solution in the dish was placed in a muffle furnace at temperature 400±10 ºC. After complete combustion, a porous white preform of ZnO was obtained. In the present system, oxidizer to fuel ratio was varied to obtain high crystalline ZnO sponges. A series of experiments are conducted in respect of crystal structure, morphology and surface area. The reaction inside muffle furnace is shown in Figure 5. The powders obtained were analytically characterized using the techniques explained below. A simple flowchart of the synthesis has been shown in Figure 6.

Figure 5. Combustion reaction is taking place in crystallization dish.

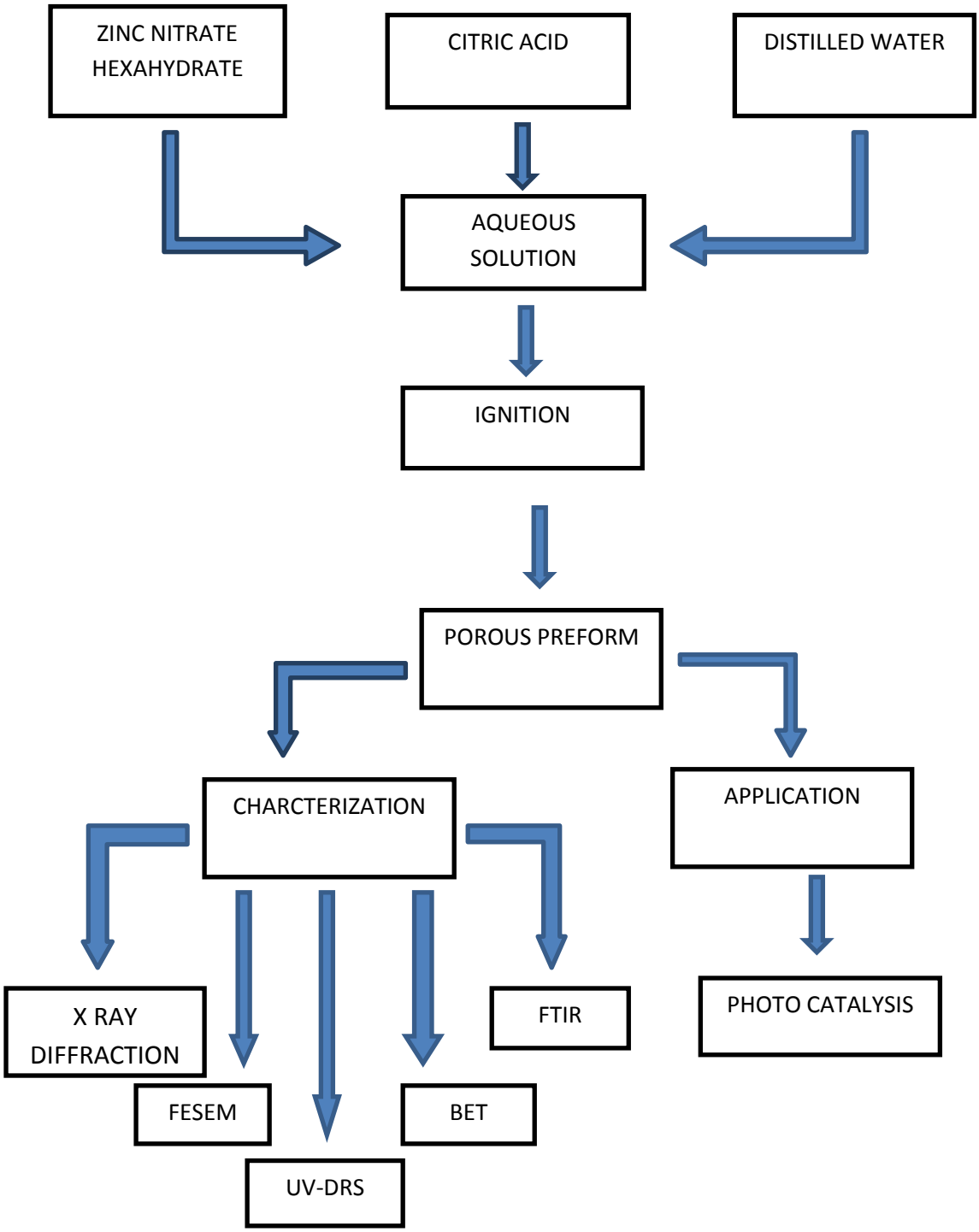

Figure 6. Flowchart for the synthesis of spongy-ZnO.

3.2. Analytical Characterizations

3.2.1. X-Ray Diffraction

XRD is a rapid and non-destructive instrumental technique to determine the phase of the crystalline material. X- Ray beam generated when an electron beam strikes an anode in a sealed tube. These X-Ray beams are projected on the sample where a part of the beam is transmitted, reflected, refracted and gets absorbed. Braggs law gives the condition for constructive interference required to find inter atomic spacing of sample. X- ray diffraction (XRD) pattern for all the powders was obtained using a Rigaku Ultima IV X-ray diffractometer with Ni filtered K_α radiation (λ=1.5418 Aº) as shown in Figure 7.

Figure 7. The image of Rigaku Ultima IV X-Ray Diffractometer.

3.2.2. Field Emission Scanning Electron Microscopy (FESEM)

Field emission scanning electron microscopy uses electron beam instead of light to visualize specimen's surface with a high-resolution imaging and a minimum damage to the surface at very low accelerating voltages. The samples are mounted on carbon tape paste on a stub followed by golf sputter coating. This technique is used for dimensional analysis, process characterization, particle size identification and also microstructural analysis. Here in this experiment, this technique is used for identification of particle sizes and dimensions of different samples. FESEM images of ZnO powder was carried out using NOVA NANOSEM FEI 450 system as shown in Figure 8.

Figure 8. Digital image of NOVA NANOSEM FEI 450 system.

3.2.3. Fourier Transform Infra-Red Spectroscopy (FT-IR)

Fourier transforms infrared spectroscopy is used to check the absorbance, emission and photon conductivity of a solid, liquid or a gas sample. FTIR principle based upon the principle that most molecules absorb light in the infrared region of electromagnetic spectrum. This measurement uses small specimen discs that are prepared using KBr as reference material. A homogeneous mixture of KBr and material is prepared by mixing the powders using mortar and pestle. The homogeneously mixed powder is then pelletized using pelletizer under 3-ton pressure. The image of the Perkin Elmer FTIR spectrophotometer instrument is given in Figure 9.

Figure 9. The image of Perkin Elmer FT-IR spectrophotometer.

3.2.4. Brunauer–Emmett-Teller (BET) Analysis

Brunauer, Emmett and Teller technique is used to explain the theory of physical adsorption of the gas molecule on a solid surface and describes specific surface area of the sample. This

theory is an extension of Langmuir theory with the following hypothesis: (a) there is physical adsorption of gas molecules in a solid surface. (b) There is no reaction between the gas molecules and solid surface. (c) Monolayer adsorption can take place over multilayer adsorption. This technique is used for characterisation of disperse, macroporous materials (pore diameter >50nm), mesoporous materials (pore diameter between 2-50nm) and microporous materials (pore diameter <2nm). The typical BET set up is shown in Figure 10.

Figure 10. The image of BET apparatus for measuring the surface area.

3.2.5. UV-Vis Diffuse Reflectance

Ultra Violet – Visible diffuse reflectance spectroscopy (Figure 11) is used to study absorption spectroscopy in ultraviolet-visible spectrum region. The principle of this technique is that light is absorbed by molecules containing π-electrons that excite valance electron to higher anti-bonding molecular orbital. Barium sulfate is taken as reference material.

Figure 11. The image of Shimadzu UV-Visible Spectrophotometer.

3.3. Photocatalytic Experiments

Methyl violet has been taken as a model dye for photocatalytic experiments. The structure of methyl violet dye is shown in Figure 12. A standard methyl violet solution of 10 ppm was made by diluting 100ppm solution of methyl violet in distilled water. 30 ml of 10 ppm methyl violet solution with 30 mg of catalyst was suspended in a Pyrex reactor. The catalyst concentration of 1 g/l was maintained throughout the solution. The dye solution along with the catalyst was stirred on a magnetic stirrer for 60 minutes to maintain the equilibrium of absorption and desorption. At certain time intervals, 5 ml dye along with catalyst solution was taken out and centrifuged at 3000 rpm for 10 min to separate the catalyst from dye catalyst solution. The change in concentration causes a change in absorbance that is detected by UV-visible spectrometer [27]. The absorbance maximum for methyl violet is at 590 nm.

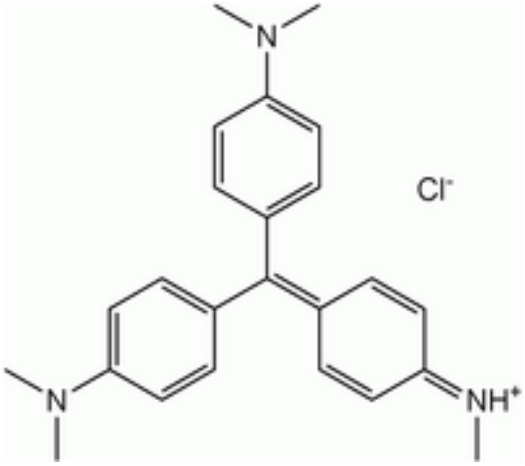

Figure 12. The structure of Methyl Violet Dye.

Chapter-4

Results & Discussion

4.1. Phase Analysis

Phase analyzes of spongy-ZnO powders synthesized with a different oxidizer to fuel ratio are carried through X-ray diffraction patterns as shown in Figure 13-15. Initially, the experiments were performed by taking the fuel deficient, stoichiometric and fuel excess concentration of both oxidizer and fuel for 30 min at 400^{o}C. The XRD patterns of fuel deficient, stoichiometric and fuel excess is shown in Figure 13-15, respectively. The porous mass obtained from deficiency of fuel shows an impurity peak due to incomplete combustion reaction as shown in Figure 13. This peak has been identified as zinc nitrate and marked in the figure as '#'. This is a low purity zinc oxide powder and is brown in color due to the presence of carbonaceous matter in it.

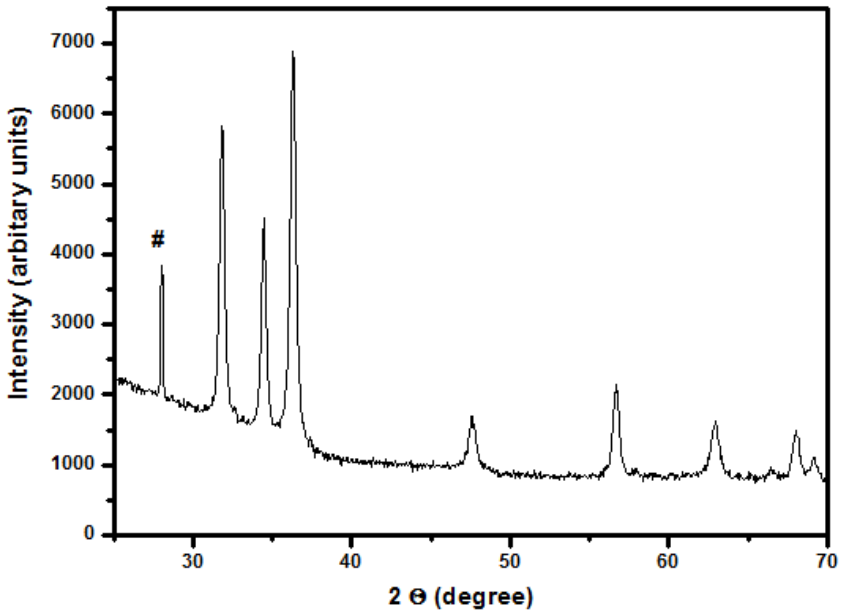

Figure 13. XRD pattern of spongy ZnO with fuel deficiency.

However, it is observed that stoichiometric ratio and excess of fuel produces hexagonal wurtzite structure. There is the difference in crystallinity as seen in Figure 14 and

Figure 15. This hexagonal crystal phase matches well with JCPDS No. –79-0206. Indexing of the peak has been done to Figure 15 with planes (100), (002), (101), (102), (110), (103), (200) and (112) that corresponds to the hexagonal crystal phase.

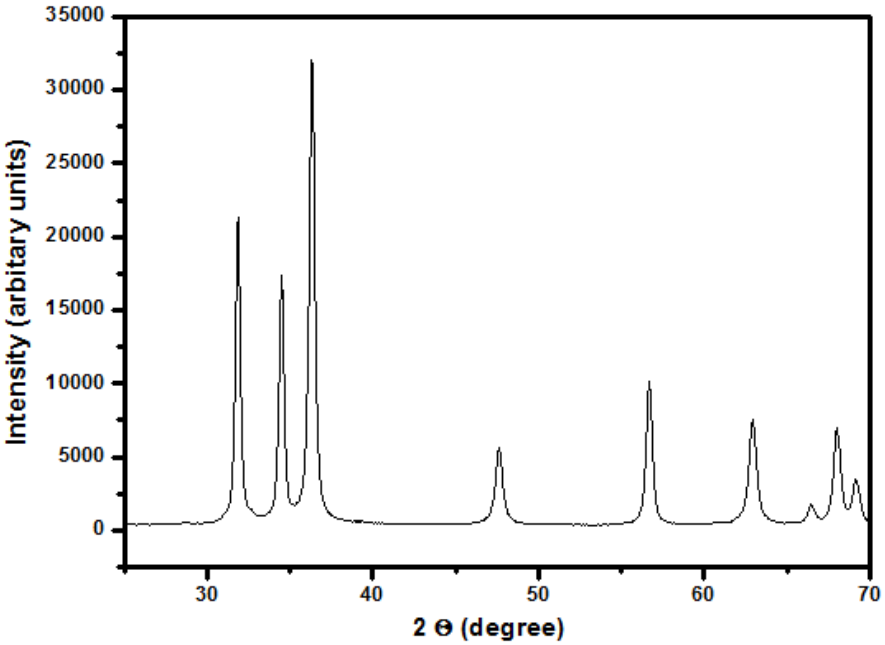

Figure 14. XRD pattern of spongy ZnO with the stoichiometric ratio.

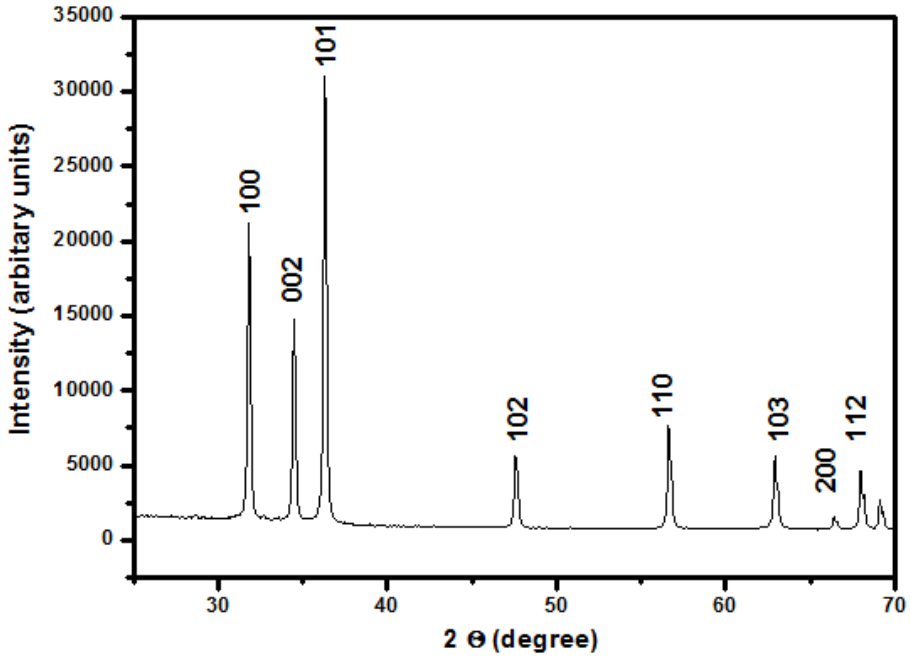

Figure 15. XRD pattern of spongy ZnO with fuel excess.

4.2. Functional Group Analysis

The spongy ZnO nanopowders obtained from the stoichiometric concentration of oxidizer and fuel has been considered for evaluation of functional groups. Figure 16 shows the FT-IR pattern of optimized spongy-ZnO. There are several depression as observed in the figure that corresponds to an absorption peak and is resulted due to the vibration of various functional groups. There is a depression peak at wavenumber 520 cm^{-1} that attributes to the vibration of Zn-O group. A broad absorption peak at wavenumber 3300 cm^{-1} is responsible due to the vibration of O-H group of the water molecule that are physically and chemically adsorbed over the powder surface. Asymmetric and symmetric stretching of carboxylic groups contributes a small peak absorbance at wavenumbers near to 1587 cm^{-1} and 1398 cm^{-1}. Hence, FT-IR spectroscopy confirms that some functional groups like CO and OH groups is obtained that corresponds to trance amount of carbon [28].

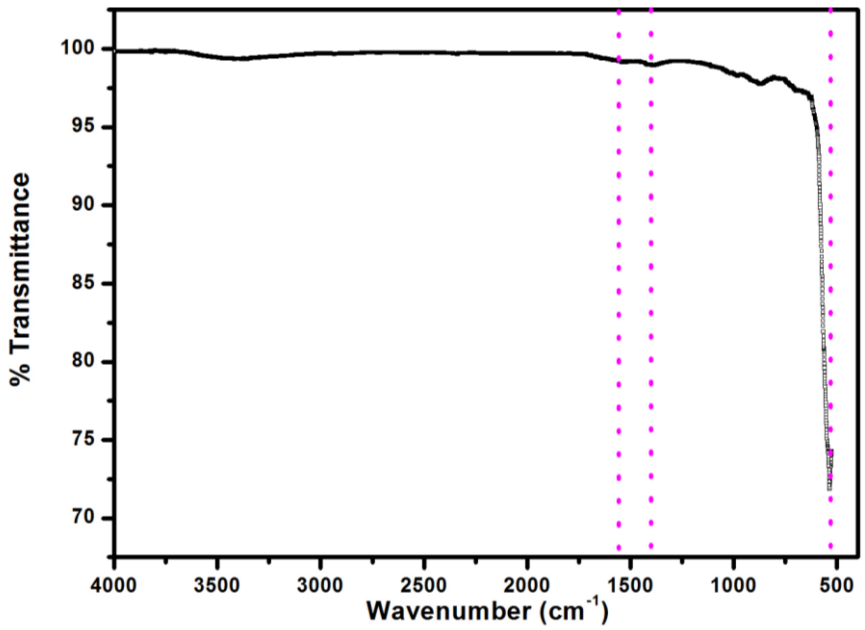

Figure 16. XRD pattern of spongy ZnO with fuel excess.

4.3. Morphological Analysis

The low resolution and high-resolution FESEM images of spongy-ZnO from optimized oxidizer to fuel ratio has been carried and presented in Figure 17 and Figure 18, respectively. The reaction proceeded with the formation of gel-like structure upon boiling when inside the furnace. Figure 17 shows that the zinc oxide obtained via combustion process is highly porous and fluffy in nature. Close viewing shows that the porous mass is forming sponge-like structure. Thus, zinc oxide has been designated as spongy-ZnO. High-resolution FESEM image shows that small near spherical particles are agglomerated and clustered to form sponge-like structure. Since, the reaction is highly exothermic and rapid, particle grows and forms a cluster. The average particle size as calculated from the FESEM image is found to be 55 nm.[29] The measured BET surface area of the spongy-ZnO is 19.2 m^2/g.

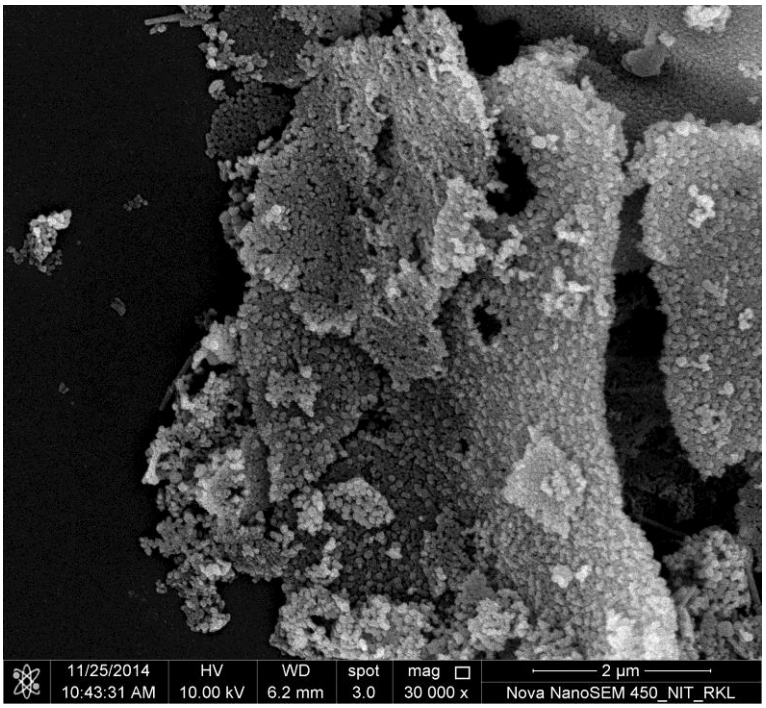

Figure 17. Low-resolution FESEM image of spongy-ZnO.

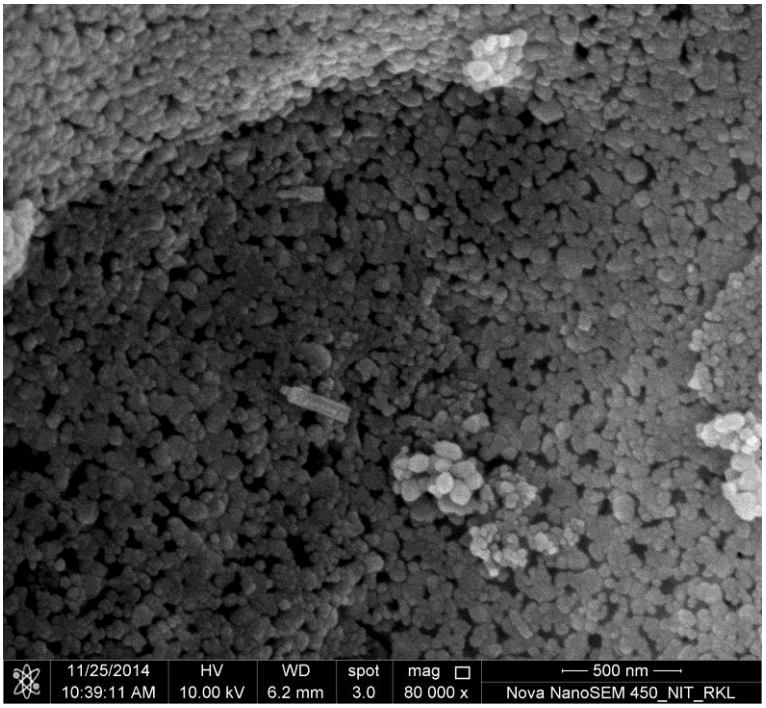

Figure 18. High-resolution FESEM image of spongy-ZnO.

4.4. UV-DRS and band gap measurement

Diffuse reflectance spectrometer is used to measure the optical properties and band gap of optimized spongy-ZnO powder. The diffuse reflectance spectrum of ZnO is shown in Figure 19. In order to calculate band gap energy values from diffuse reflectance spectra, Kubelka-Munk relationship is used. The kubelka-munk relation is given by $F(R) = (1-R^2)/2R$ where R is reflectance [30]. Multiplication of square root of F(R) is plotted against photon energy ($h\upsilon$) and it slope gives band gap energy (Tauc plot) as shown in Figure 20. Band gap value for ZnO is found to be 2.75 eV from Tauc plot. The band gap is found to decrease from the bulk value 3.2 eV due to the size of the particle found to be in nanosized range. The band gap value obtained is in correspondence to the literature reported values [31].

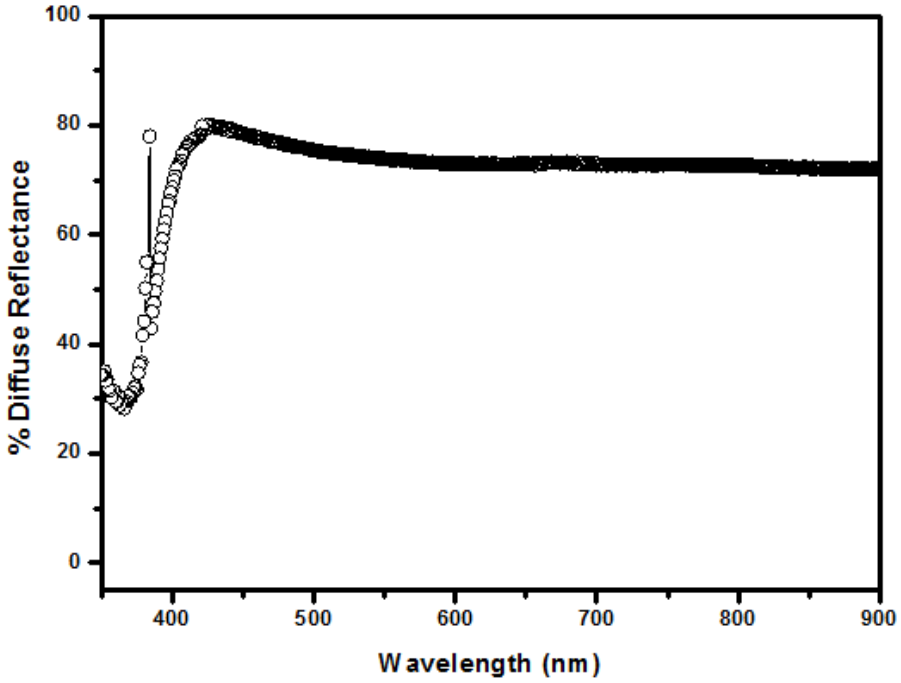

Figure 19. UV-Diffuse reflectance spectra of spongy-ZnO.

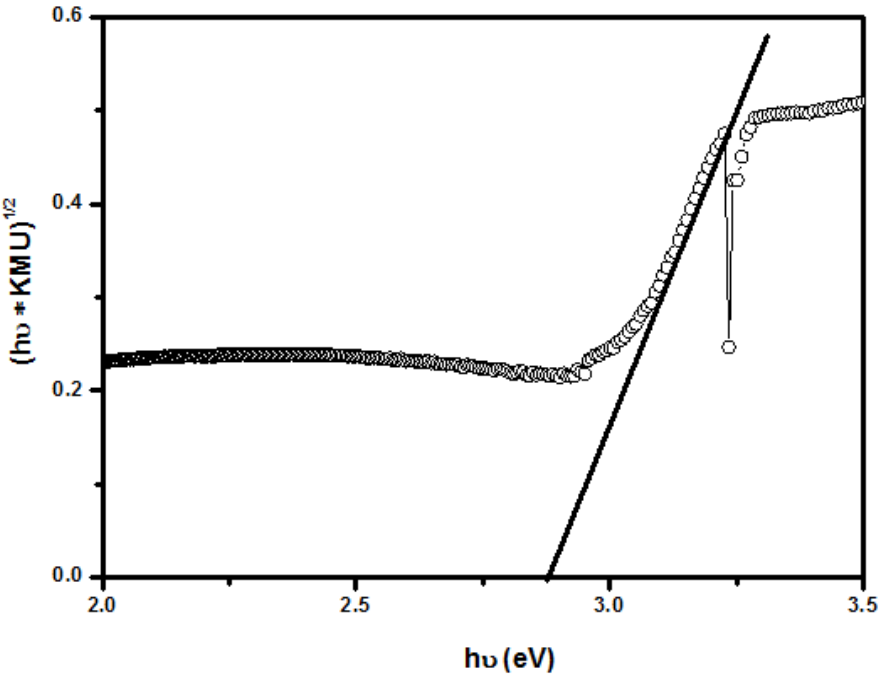

Figure 20. Band gap energy from Tauc plot.

4.5. Photocatalysis

One of the characteristics of ZnO is that it can act as an active catalyst and reduce the concentration of methyl violet by photochemical reaction under the influence of visible lights. Methyl violet ($C_{23}H_{26}N_3$) is a used as a pigment in textile industries. Water bodies get contaminated by this dye and also it is harmful to human activity. Therefore, the synthesized spongy-ZnO is used to photocatalytically degrade this dye in the presence of light radiation. Figure 21 shows the degradation profile of methyl violet degradation for 60 min with 10 min intervals. Degradation profile is given by C/C_0 plotted against degradation time interval. C represents the concentration of methyl violet till exposure time (t) and C_0 represents the initial concentration of standard methyl violet. Photolysis of methyl violet under visible light gives only 9% degradation in the concentration of methyl violet. Hence, ZnO is used as a catalyst to further enhance the degradation [32].

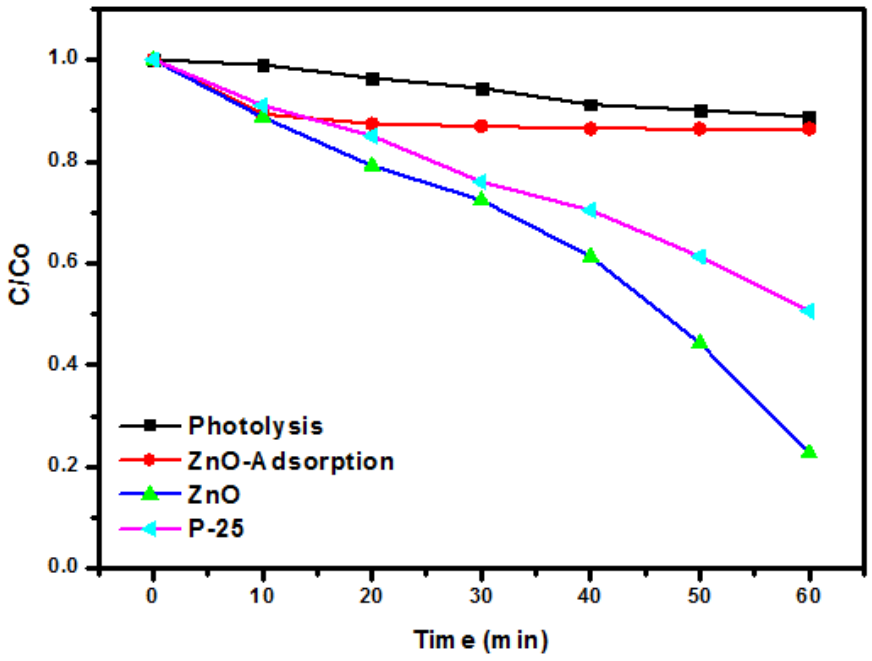

Figure 21. Degradation profile of methyl violet using spongy-ZnO.

With wide band gap and large exciton binding energy, upon irradiation of visible light, zinc oxide produces oxidizing species to reduce the concentration of methyl violet. When ZnO is irradiated under the visible light it shows degradation up to 80% after 60 minutes which is more than that of commercially available P25 TiO_2 that shows only 45% degradation. The sponge-like structure and high surface area of zinc oxide provides more active sites for a photochemical reaction. We can conclude that spongy-ZnO act as a more effective catalyst with increased efficiency [33].

Chapter-5
Conclusion

- Summarizing the thesis, hexagonal wurtzite spongy-ZnO has been successfully synthesized by a novel one-step solution combustion method in presence of the fuel citric acid.
- XRD pattern confirms the hexagonal crystal phase for powders synthesized under stoichiometric conditions. However, fuel deficient during combustion process lead to incomplete combustion of zinc nitrate that was evident from the phase analysis.
- The spongy, fluffy and porous structure of ZnO is observed where the particles are seen clustered due to rapid exothermic process and has average particle size near to 55nm. The surface area measured for zinc oxide is 19.2 m^2/g.
- The presence of trace amount of carbonaceous matter is observed and confirmed from FT-IR spectral analysis. The band gap energy is calculated from Tauc plot and the value obtained is 2.75eV.
- Photocatalytic degradation of methyl violet under visible light irradiation is carried and 80% degradation is obtained due to large number of active sites present in the sponge structure. The above results pacify that combustion synthesized spongy-ZnO act as an efficient photocatalyst.

REFERENCES

1) D. Beydoun, R. Amal, G. Low and S. McEvoy, Journal of Nanoparticle Research 1(4), 1999, 439–458.

2) W. Wu, C. Jiang and V. A. L. Roy, Nanoscale, 7, 2015, 38-58.

3) Z. L. Wang and J. Song, Science. 312, 2006, 242-245.

4) S. M.Samuel, L. Bose and George, Academic Review, 16, 2009, 57-65.

5) G. V. Elmore, H. A. Tanner, J. Phys. Chem., 60 (9), 1956, 1328–1329.

6) A. B. Djurišić, A. M. C. Ng, X. Y. Chen, Progress in Quantum Electronics, 34(4), 2010, 191-259.

7) M. Caglara, S. licana, Y. Caglara, F. Yakuphanoglub, Physica, E 35, 2006, 131–138.

8) S K Gupta, A. Joshi and M. Kaur, J. Chem. Sci., 122, 2010, 57–62.

9) Y.H. Hsu, J. Lin, W. C. Tang, Mater Electron, 19, 2008, 653–661.

10) L. Saad and M. Riad, J. Serb. Chem. Soc. 73 (6), 2008, 997–1009

11) A. K. Radzimska and T. Jesionowski, Materials, 7, 2014, 2833-2881

12) S. Shishiyanu, L. Chow, O. Lupan, and T. Shishiyanu, ECS Transactions, 3 (9), 2006, 65-71.

13) M. Vaseem, A. Umar, Y.B Hahn, ZnO Nanoparticles: Growth, Properties, and Applications, American Scientific Publishers.

14) Z. L.Wang, Condens Matter, 16, 2004, 829–858.

15) P. A. Rodnyi and I. V. Khodyuk, Optics and Spectroscopy, 111(5), 2011, 776-785.

16) C. Chen, J. Liu, P. Liu, B. Yu, Advances in Chemical Engineering and Science, 1, 2011, 9-14.

17) B. Neppolian, H.C. Choi, S. Sakthivel, B. Arabindoo, V. Murugesan, Hazardous Materials, 89, 2002, 303–317.

18) S. S. Kumar, P. Venkateswarlu, International Nano Letters, 3, 2013, 30-36.

19) S. T. Aruna, A. S. Mukasyan, Current Opinion in Solid State and Materials Science 12, 2008, 44–50

20) R. Ianos, I. Lazˇaua, C. Pˇacurariua, P. Sfirloag, Materials Chemistry and Physics 129, 2011, 881– 886.

21) C.C. Hwang, T.Y. Wu, J. Mater. Sci. 39, 2004, 6111–6115.

22) C.C. Hwang, T.Y. Wu. Materials Science and Engineering, B 111, 2004, 197–206.

23) P. R. Potti and V. C. Srivastava, Ind. Eng. Chem. Res, 51, 2012, 7948−7956.

24) R. Nagaraja, N. Kottam , C.R. Girija, B.M. Nagabhushana, Powder Technology 91, 2012, 215-216.

25) S. Adhikari, D. Sarkar and G. Madrasb, RSC Advances, 4, 2014, 55807–55814.

26) S. K. Sharma, S. S. Pitale, M. Manzar Malik, R. N. Dubey, M. S. Qureshi, S.Ojha, Physica B, 405, 2010, 866-874.

27) J. Coates, Interpretation of Infrared Spectra, A Practical Approach, John Wiley & Sons Ltd.

28) S.L. Upstone, Ultraviolet/visible light absorption spectroscopyin clinical chemistry, John Willey & Sons Ltd.

29) N. P. Mohabansi, V. B. Patil and N.Y. Rasayan, J .Chem, 4(4), 2011, 814-819.

30) S. Sun, X. Yang, Y. Zhang, F. Zhang, J. Ding, J. Bao and C. Gao, Progress in Natural Science 22(6), 2012, 639–643.

31) B. Li and Y. Wang, J. Phys. Chem C., 114, 2009, 890-896.

32) Z. Deng, M. Chen, G. Gu and L. Wu, J. Phys. Chem. C, 112, 2007, 16-22.

33) A. Gharib, N.N. Pesyan, L.V. Fard and M. Roshani, J. Chem. Eng. Chem. Res. 1, 2014, 1-5.